An early *Australopithecus afarensis* postcranium from Woranso-Mille, Ethiopia

Yohannes Haile-Selassie[a,b,c,1], Bruce M. Latimer[a,b,c], Mulugeta Alene[d], Alan L. Deino[e], Luis Gibert[e], Stephanie M. Melillo[f], Beverly Z. Saylor[g], Gary R. Scott[e], and C. Owen Lovejoy[a,h,1]

[a]The Cleveland Museum of Natural History, Cleveland, OH 44106; [b]Department of Anthropology, [c]The Institute for the Science of Origins, and [g]Department of Geological Sciences, Case Western Reserve University, Cleveland, OH 44106; [d]Department of Earth Sciences, Addis Ababa University, Addis Ababa, Ethiopia 1176; [e]Berkeley Geochronology Center, Berkeley, CA 94709; [f]Department of Biology, Stanford University, Stanford, CA 94305; and [h]Department of Anthropology, School of Biomedical Sciences, Kent State University, Kent, OH 44242

Contributed by C. Owen Lovejoy, April 16, 2010 (sent for review February 22, 2010)

Only one partial skeleton that includes both forelimb and hindlimb elements has been reported for *Australopithecus afarensis*. The diminutive size of this specimen (A.L. 288-1 ["Lucy"]) has hampered our understanding of the paleobiology of this species absent the potential impact of allometry. Here we describe a large-bodied (i.e., well within the range of living *Homo*) specimen that, at 3.58 Ma, also substantially antedates A.L. 288–1. It provides fundamental evidence of limb proportions, thoracic form, and locomotor heritage in *Australopithecus afarensis*. Together, these characteristics further establish that bipedality in *Australopithecus* was highly evolved and that thoracic form differed substantially from that of either extant African ape.

bipedality | human evolution | upright walking | hominid | thorax

Since the first recognition of *Australopithecus afarensis* (see below) only one partial skeleton with both forelimb and hindlimb elements has been reported [A.L. 288–1 ("Lucy")]. The specimen's unusually small body size has raised issues of allometry. Here we describe a moderately large-bodied (i.e., well within the range of living *Homo* in many aspects) partial skeleton, KSD-VP-1/1 (Fig. 1). It provides evidence of limb proportions, thoracic form, and locomotor heritage in hominids (i.e., specimens in the human clade postdating separation from the chimpanzee/bonobo clade).

Discovery and Preservation

KSD-VP-1/1 was found in mudstone at the base of an exposure of upward-coarsening claystone, siltstone, and sandstone. The first element, a proximal ulna, was found by Alemayehu Asfaw on February 10, 2005, from Korsi Dora vertebrate locality 1 (KSD-VP-1) in the Woranso-Mille paleontological study area of the Afar region, Ethiopia (*SI Appendix*, Fig. S1). Crawling and surface scraping resulted in the recovery of more parts of the ulna, the distal half of the femur, cervical vertebrae, humeral shaft fragments, and a partial sacrum. Excavation of the locality resulted in the in situ recovery of an os coxa, tibia, clavicle, five ribs, and a scapula. No cranium or dentition was recovered (*SI Appendix*, Table S1).

Stratigraphy and Age

The Woranso-Mille paleontological study area lies within the western part of the central Afar depression (1–3) (*SI Appendix*, Fig. S1). Exploration began in 2002, and more than 4,300 fossil specimens (including 95 from hominids) have been collected thus far from 55 vertebrate localities (2). The stratigraphy and age relationships of its northwestern part are relatively well understood and are temporally well constrained (2, 3). However, the specimen's specific locality, KSD-VP-1, is isolated from known stratigraphy by a normal fault trending northwest–southeast. Fortunately, it has been possible, through radiometric dating and paleomagnetic reversal stratigraphy, to constrain the age of this isolated block to *ca.* 3.60–3.58 Ma (*SI Appendix*, Figs. S2–S5 and Table S2).

Taxonomy

KSD-VP-1/1 antedates A.L. 288–1 (4) by roughly 0.4 Ma and is generally contemporaneous with specimens from Laetoli (including the type specimen) (5). Although the absence of cranial and dental elements imposes some restrictions on the specimen's taxonomic assignment, it shares a substantial number of postcranial elements with homologs in A.L. 288–1. These elements are fundamentally similar in morphology to A.L. 288–1 and are sufficient to warrant attribution to *Australopithecus afarensis*. Differences appear to result largely from body size and sex. Details of the KSD-VP-1/1 pelvis suggest that it is male (see below). A.L. 288–1 is almost certainly female (6) (*contra* 7).

Hindlimb

KSD-VP-1/1d is a right os coxa, including an acetabulum, a superior ischial ramus, the dorsal half of the ischial tuberosity, and much of the ilium inferior to the crest (*SI Appendix*, Fig. S6). An articulating first sacral segment also was recovered (*SI Appendix*, Fig. S7).

The os coxa has suffered numerous fossilization cracks, but fragments have been retained in good alignment. However, portions of the retroauricular area, including the posterior superior iliac spine (PSIS) have undergone substantial postmortem translation and repositioning superiorly and anteriorly (*SI Appendix*, Fig. S6). This region provides only limited anatomical information save that the PSIS was robust.

The pelvis exhibits a "classic" *Australopithecus* pattern (*SI Appendix*, Table S3) with which it shares numerous features, including a voluminous obturator externus tendon groove isolating the inferior acetabular wall from the ischium and a distinct dorsal (hamstring) portion of its ischial tuberosity that faces superolaterally in modern humans (8–11) but not in *Ardipithecus ramidus* (9) or African apes. The groove's breadth is somewhat greater than in *Homo* (*SI Appendix*, Fig. S8 and Table S3) but is dramatically reduced as compared with that of *Ar. ramidus* (9). Further details are provided in *SI Appendix*, Note S2.

The sacrum also conforms to the *Australopithecus* pattern. Its auricular surface is narrow, as in A.L. 288–1 and Sts 14, and shows broad sacral alae relative to centrum size (*SI Appendix*, Fig. S10). The dorsal alar tubercle is difficult to assess because of damage, but surrounding bone suggests that it was absent or gracile, as in A.L. 288–1 (12). In contrast, the postauricular region of the os coxa is rugose, suggesting extensive posterior reinforcement of the joint (*SI Appendix*, Fig. S6). The narrowness

Author contributions: Y.H.-S., B.M.L., M.A., A.L.D., L.G., B.Z.S., G.R.S., and C.O.L. designed research; Y.H.-S., B.M.L., M.A., A.L.D., L.G., S.M.M., B.Z.S., and C.O.L. performed research; Y.H.-S., B.M.L., M.A., A.L.D., L.G., B.Z.S., G.R.S., and C.O.L. analyzed data; and Y.H.-S., B.M.L., A.L.D., L.G., B.Z.S., and C.O.L. wrote the paper.

The authors declare no conflict of interest.

[1]To whom correspondence may be addressed. E-mail: olovejoy@aol.com or yhailese@cmnh.org.

This article contains supporting information online at www.pnas.org/lookup/suppl/doi:10.1073/pnas.1004527107/-/DCSupplemental.

Fig. 1. Anatomically arranged elements of KSD-VP-1/1. A list of all elements is provided in *SI Appendix*, Table S1.

and inferior location of the superior terminus of the auricular surface suggest possible sacralization of the (missing) most caudal lumbar. The relatively narrow auricular surface raises the possibility that nutation and counternutation were significantly more important as energy-dissipating mechanisms in the sacroiliac joint during running in *Australopithecus* than in *Homo* (13).

KSD-VP-1/1c is a left distal femur (*SI Appendix*, Fig. S11). The lateral condyle is decidedly elliptical, although its shape index of 52 (14) places it near the maximum in a small human sample (*SI Appendix*, Table S4). It forms an elevated lateral wall for patellar retention, implying selection imposed by habitual valgus [type 1 (15); for definition see *SI Appendix*, Table S5]. A deep, well-defined, popliteus groove is present. The supracondylar lines, although damaged, when tracked proximally form a moderately elevated linea as in other *Au. afarensis* (16) (breadth = 12 mm at point of shaft fracture, 187 mm from the distal end).

A left tibia (KSD-VP-1/1e; *SI Appendix*, Figs. S12 and S13) is truncated just proximal to the tibial tuberosity but preserves the transverse groove between the shaft and plateau occupied by the fat pad/bursa beneath the patellar tendon. Along with its intact distal plafond, this distance allows an accurate estimate of maximum length (355 mm; Table S6) by simple comparison with human tibias with the same overall dimensions (tibial tuberosity to center of plafond surface). Its overall form is distinctly platycnemic, but surface features (e.g., insertion details of the pes anserinus tendons) are difficult to interpret because of cortical exfoliation.

The distal end is well preserved, although the medial malleolus has been sheared away at its base. The tibiofibular syndesmosis exhibits extensive pathology (*SI Appendix*, Fig. S12). The fibular facet's perimeter presents a "ring" of elevated, reactive bone extending medially to involve the lateral half of the anterior tibial surface. This ring has extended the shaft inferiorly by 5–10 mm (not included in its estimated length). The plafond's subchondral surface is unaffected. The most likely explanation is a remote, nonunited, preadult fibular fracture (17).

The talocrural joint's radius of curvature is among the most discriminating characters of hominoids (18–21). Human plafonds have short radii of curvature. Those of apes are much flatter (19), either permitting (type 1) or reflecting (type 4) substantial dorsiflexion during vertical climbing (in contradistinction to clambering or oblique climbing). Relative plafond depth (RPD) has a median value of 16 in humans, whereas in African apes it lies between 12 and 14 (18). The RPD for KSD-VP-1/1e is well above 20, even after correcting for its osteophytosis which artificially increases the index. Simple visual assessment, moreover, confirms an original plafond depth far greater than in any ape (*SI Appendix*, Table S7). A high RPD also characterizes at least 11 early hominid tibias (18). Additional details are provided in *SI Appendix*, Note S3.

Thorax

Hominoid pectoral structure reflects multiple parameters, including spinal column invagination, rib morphology, dimensions of the iliocostal space, and scapular form (22). KSD-VP-1/1 is the first single *Australopithecus* specimen to preserve a combination of some of these elements.

The lateral and distal portions of each human rib descend more obliquely from their vertebral origins than in African apes. Such declination increases thoracic transverse diameter and elongates the thorax (23–25). Declination also induces more flexed costal angles (each rib head is more inferiorly angled relative to its corpus), as well as torsion and flattening of each rib body, although the latter characters are highly variable. African apes lack rib obliquity, and their greatly reduced lumbar columns and iliocostal spaces prevent significant rib declination (23, 24). Their ribs exhibit more rounded cross-sections and have little or no axial torsion (24).

Five KSD-VP-1/1 ribs, although damaged, are sufficiently complete (unlike those of A.L. 288–1) to demonstrate overall fundamental structure (*SI Appendix*, Figs. S14–S17 and Table S1). They exhibit (*i*) marked costal angles indicating deeper vertebral column invagination into the thorax than in apes; (*ii*) cross-sectional flattening with deeply marked subcostal grooves and sharp inferior pleural margins; and (*iii*) axial torsion consistent with inferior declination and craniocaudal elongation. The single most distinct character of the African ape thoraces, however, is their marked cupular constriction, which is largely responsible for their description as "funnel-shaped" (see refs. 24 and 25 for discussion). The second rib (KSD-VP-1/1n) is sufficiently intact for assessment of overall form (*SI Appendix*, Fig. S16). Even though a "rib shape index" overlaps in humans and gorillas (Fig. 2 and *SI Appendix*, Fig. S17), there is little question that the upper thorax of KSD-VP-1/1 was fundamentally *Homo*-like.

KSD-VP-1/1f is most of a left clavicle (*SI Appendix*, Fig. S18). It lacks at least 10 mm from its acromial expansion and a significant portion of its sternal end. Clavicle length and midshaft circumferences show a moderately robust relationship ($r = 0.72$) (*SI Appendix*, Table S8) and suggest the specimen's length to be 156 mm [C (140 < 156 < 172) = 80%]. In a plot of clavicle length and the geometric mean of various joint dimensions of the upper limb, KSD-VP-1/1f falls within the human distribution (*SI Appendix*, Fig. S19). When its estimated clavicle length is compared with other upper limb dimensions, it falls generally with *Homo* (*SI Appendix*, Fig. S20).

No previous adult specimen of *Australopithecus* has preserved as much of the scapula as does KSD-VP-1/1g (Fig. 3). Four other

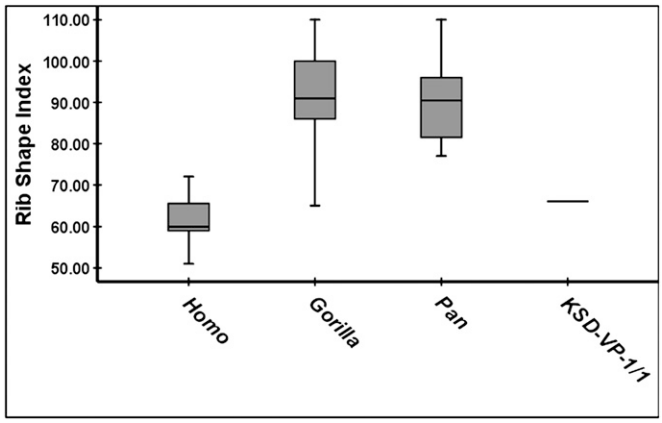

Fig. 2. Rib curvature index of the second rib. Assessment method is shown in *SI Appendix*, Fig. S17. Although one *Gorilla* specimen (CMNH-B1781)(n = 33) fell within the human range, KSD-VP-1/1n lies well within the human range. The platypelloidy of *Australopithecus* probably made its inferior thorax mediolaterally broad; but this breadth would have been unrelated to the "pyramidal form" of African ape thoraces. Box plot parameters are provided in *SI Appendix*, Fig. S8.

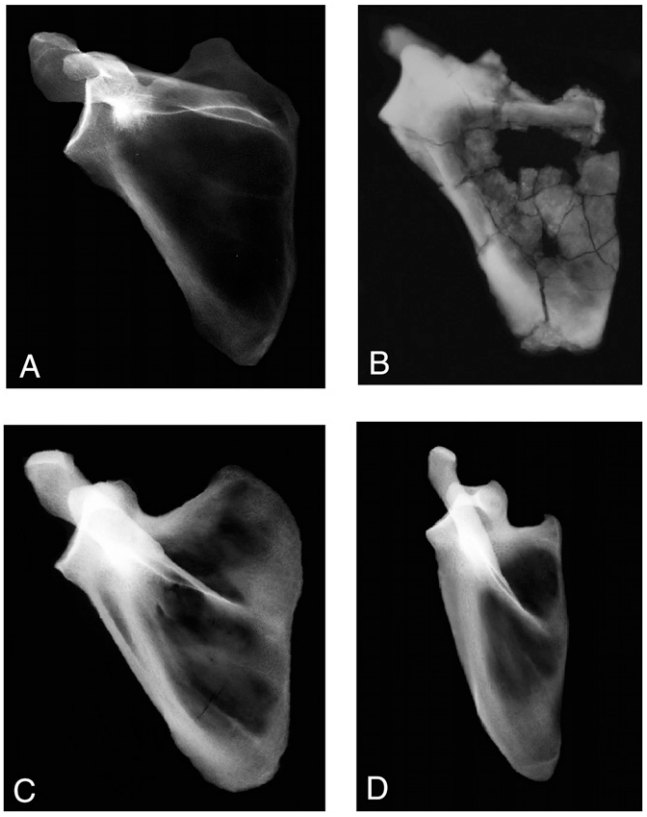

Fig. 3. X-rays of hominoid scapulas. (*A*) Modern human (CMNH-HTH-2450). (*B*) KSD-VP-1/1g. (*C*) *Gorilla* (CMNH-B-1730). (*D*) *Pan* (CMNH-B-3551). Each specimen has been scaled to the same approximate superoinferior glenoid height and aligned with its vertebral border approximately vertical. Note the uniqueness of *Pan* if a line is drawn connecting each specimen's superior and inferior angles (largely vertical in *D*). The human's glenoid angle is among the most superior in our sample (n = 21). All specimens, save *Pan*, have similar glenoid orientations. Both *Pan* and *Gorilla* are distinguished from the hominids by their substantially greater inferomedial spine orientation. KSD-VP-1/1g is most similar to humans. *Pan* is clearly the morphological outlier.

specimens [A.L. 288–1 (4), StW 162, StW 366, and Sts 7 (26)] are largely glenoid fragments with small portions of their spine and fossae. A fifth (DIK-1-1), although nearly intact, is from an infant (27). A sixth (StW 431) preserves only the axillary border (28). KSD-VP-1/1g preserves a nearly complete infraspinous fossa, the entire spine, and a complete glenoid. The acromion and coracoid are lacking. A small portion of the supraspinous fossa includes the scapular notch but is insufficient to determine the size of the fossa. The spine was bent postmortem, reducing its angle with the supraspinous fossa but with no damage to its relationship with the remainder of the bone.

The "bar–glenoid" angle has been used to orient the glenoid plane in A.L. 288–1 (29), but the specimen's small size may have had scaling effects (30, 31), an observation supported by the fact that its bar–glenoid angle can be matched exactly by comparably sized humans (*SI Appendix*, Fig. S21). Based again on glenoid plane angle, the DIK-1–1 juvenile scapula was argued to demonstrate strong affinities to *Gorilla* (27). Calculation of its glenoid angle, however, relied on a reference axis defined by the superior and inferior angles, landmarks that fluctuate substantially in *Homo sapiens* (32) and differ substantially in at least *Pan* and *Homo*. A principal components analysis (PCA) placed DIK-1–1 within a *Gorilla* distribution. However, that analysis generated only two principal components (PCs) not dominated by size (i.e., PC1 was not informative). PC3 did not discriminate among the taxa (and was trivial, accounting for <1% of the variance). Only PC2 discriminated humans from apes but accounted for <7% of the variance. Moreover, its factor loadings demonstrate only minimal effect from any variables save three largely redundant measures of relative infraspinous and supraspinous fossa area (27). A high supraspinous/infraspinous ratio certainly is expected in any species with an arboreal heritage (*SI Appendix*, Fig. S22) but is unlikely to be probative for the pectoral girdle's total morphological pattern (33).

It is potentially more informative to explore geometric relationships within the bone's primary infrastructure, i.e., the relative spatial orientations of its glenoid plane (glenohumeral joint function), axillary border (rotator cuff), spine (trapezius, infraspinatus, and supraspinatus), and vertebral border (rhomboids and serratus anterior). KSD-VP-1/1g allows accurate calculation of five angles that should reflect these functional relationships (Table 1 and *SI Appendix*, Fig. S23). KSD-VP-1/1g is within the human and chimpanzee size ranges; therefore, allometry should not be a confounding issue.

All five angles recorded in Table 1 are significantly correlated (Table 2), but none is an obvious redundant vicar of another, save bar–glenoid and axillary–glenoid, whose coefficient is close to 0.9. Some have argued that the bar–glenoid angle should reflect scapular orientation reliably (34), but it is correlated only moderately with the spino–glenoid angle (Table 2). This observation is notable, because scapular functional integration primarily reflects relationships among its blade, spine, and glenoid (35).

Comparison of KSD-VP-1/1g with other hominoid scapulas suggests functional uniqueness. In the two redundant angles (axillary–

Table 1. Angular data for the scapular angles in hominoids*

Taxon	*N*	Axillary–vertebral	Glenoid–spine	Axillary–spine	Axillary–glenoid	Bar–glenoid
H. sapiens	11	39.2 (3.0)	98.2 (5.4)	53.4 (6.5)	137.4(5.5)	140.1 (4.4)
P. troglodytes	10	29.0 (8.6)	88.2 (5.3)	28.0 (4.4)	118.4 (5.2)	124.4 (6.1)
G. gorilla	10	31.2 (8.9)	88.9 (7.0)	29.9 (5.0)	123.4 (4.9)	129.3 (6.1)
KSD-VP-1/1		31	104	50	128	134

*For a definition of each angle, see *SI Appendix*, Fig. S13.

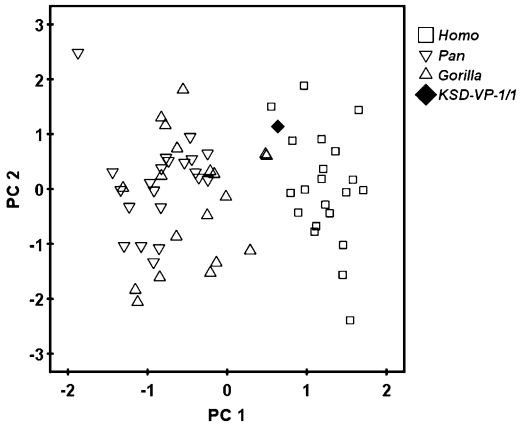

Fig. 4. PCA of scapular angular data. *PC1* for five scapular angles (schematic is shown in *SI Appendix*, Fig. S23) discriminates humans from African apes but especially from *Pan*. KSD-VP-1/1g falls within the human cloud. The standardized distance (here the univariate equivalent of the Mahalanobis D^2) between African apes and humans is very large at 4.09. PC1 is most heavily influenced by the axillary–spine and axillary–glenoid angles (Table 3). Repeating the analysis using variance-covariance rather than correlations increases D^2 to 4.57. PC2 and PC3 did not discriminate humans from apes. These data suggest that scapular spine orientation is a principal discriminator of pectoral function in humans and African apes, whereas glenoid orientation is a poorer discriminator.

glenoid and bar–glenoid), KSD-VP-1/1g is largely intermediate between humans and *Gorilla* but lies above the latter's interquartile range (*SI Appendix*, Fig. S24). Its axillary–vertebral angle is more ape-like than human-like but is a poor discriminator (Table 1). Conversely, the value of the glenoid-spine angle in KSD-VP-1/1g greatly exceeds those of African apes and even most humans (Table 1). The most powerful discriminator is the axillary–spine angle (*SI Appendix*, Fig. S25). For this measure KSD-VP-1/1g falls well within the human distribution—far above those of the African apes.

Data reduction via PCA robustly distinguishes the scapulas of humans from those of apes (Fig. 4), but two *Gorilla* specimens fall close to humans. These data suggest that some DIK-1–1 metrics are similar to those of *Gorilla* because they share a relatively large supraspinous area (27). Notably the remaining two significant components, most heavily influenced by the glenoid-spine (PC2) and axillary–vertebral (PC3) angles, are nondiscriminators. All five angles appear to influence PC1 substantially (i.e., factor loadings from 0.644 to 0.920) (Table 3), on which KSD-VP-1/1g falls within the human cloud. Moreover, the specimen plots substantially distant from any specimen of *Pan,* its closest nonhominid phyletic relative, consistent with that taxon's highly derived locomotor skeleton (22). Overall, current data therefore suggest that *Australopithecus* morphology in some ways was shared with *Gorilla* [a larger supraspinous fossa (as in DIK-1-1) (27) and a more superiorly oriented glenoid], but in others was decidedly more *Homo*-like, i.e., a scapular architecture whose total morphological pattern was unique and remarkably distant from that of *Pan*. Importantly, as also suggested by the second rib, there is clearly no evidence that the early hominid thorax was "funnel-shaped" as previously claimed (36). To the contrary, its pectoral girdle appears to reflect either a long heritage of "post-arboreal" evolution or derivation from a unique locomotor pattern not represented by any extant large-bodied hominoid, or both. Moreover, KSD-VP-1/1's greater similarity to *Homo* and *Gorilla* suggests that the pectoral girdle of *Pan* is highly derived, as suggested by data from *Ar. ramidus* (22).

Forelimb

KSD-VP-1/1b is the distal end plus two thirds of the shaft of a right humerus (*SI Appendix*, Fig. S26). It has suffered extensive exfoliation, although it clearly exhibits a typically hominid rugose deltopectoral crest (22). The trochlea and capitulum are largely preserved but with some cortical exfoliation. Estimates of distal articular surface breadth probably are accurate to within 1 or 2 mm (maximum, ≈ 48) (*SI Appendix*, Table S9). The distal end is robust, as in MAK-VP-1/2 (37) and specimens from Hadar (38).

KSD-VP-1/1a is the proximal 60% of a well-preserved right ulna (*SI Appendix*, Fig. S26). Articulation with KSD-VP-1/1b shows no significant "carrying angle." The ulnar tuberosity is well preserved and is most similar to those of humans. Shaft curvature is minimal. Although proximal elbow morphology is conservatively shared among extant hominoids, a salient exception is the orientation of the trochlear notch, which is strongly retroflexed in apes (i.e., faces superiorly) but not in early hominids (39–41). An anterior-facing notch reflects transarticular load bearing in a variety of flexed postures, whereas a more superiorly facing notch likely reflects differential loading during suspension (41). The trait in KSD-VP-1/1a is similar to its expression in A.L. 288–1 and ARA-VP-6/500 (22) (*SI Appendix*, Fig. S27 and Table S10). The specimen lacks a flexion tubercle (22).

Body Size and Dimorphism

Body size and skeletal dimorphism in *Au. afarensis* have been addressed previously (42, 43). A human regression for femoral head diameter (FHD) from acetabular diameter (44) in KSD-VP-1/1 yields 41 mm. Reno et al. (43) used ratio data from A.L. 288–1 to estimate FHD in a number of *Au. afarensis* specimens. Two undamaged sites shared by KSD-VP-1/1 and A.L. 288–1 [ulnar mediolateral breadth below the radial facet and anteroposterior articular length of the tibial plafond (43)] each yield an FHD of 36 mm for KSD-VP-1/1. These three estimates average 38 mm, making KSD-VP-1/1 the 4th largest of 16 specimens from all non-333 localities, 12th of 26 specimens from A.L. 333, and 16th among 42 possible estimates from all known specimens. The first of these rankings is probably the most representative, because individuals at 333 may have contributed multiple anatomical sites, thereby potentially skewing FHD distribution in favor of one or a few individuals. KSD-VP-1/1's position among these rankings suggests it was male.

Relative Hindlimb/Forelimb Size in Early *Australopithecus*

To date, only A.L. 288–1 (4) has been sufficiently complete to compare upper and lower limb metrics without reliance on statistically based speculation (42). Its diminutive size (43) has led to decades of contentious conjecture about the confounding effects of allometry (45, 46). The more recent A.L. 438–1 is substantially larger but lacks any hindlimb elements (40). The size of StW 573 (*Australopithecus* sp.) (47) makes it equally unlikely to resolve issues of allometry. Moreover, its attribution to an age equal to *Au. afarensis* is confounded by "many factors [that] could contribute to dating error" (p. 609, ref. 48). Analyses using ^{238}U-^{206}Pb meas-

Table 2. Correlations between scapular angles among hominoids*

	Axillary–vertebral	Glenoid–spine	Axillary–spine	Axillary–glenoid
Spino–glenoid	0.421			
Axillary–spine	0.542	0.598		
Axillary–glenoid	0.475	0.415	0.824	
Bar–glenoid	0.525	0.322	0.740	0.897

*All correlations are significant at $P < 0.0001$ except for bar–glenoid/glenoid–spine, for which $P < 0.005$ ($n = 3$).

Table 3. Principal component loadings of scapular angular data in hominoids

Variable	PC1 (67%)	PC2 (16%)	PC3 (12%)
Axillary–vertebral	0.706	0.229	0.670
Glenoid–spine	0.640	0.699	−0.281
Axillary spine	0.919	0.021	−0.170
Axillary–glenoid	0.911	−0.311	−0.153
Bar–glenoid	0.880	−0.392	0.003

urements on speleotherms suggest a recent age (2.2 Ma) (49), which is consistent with the deposit's faunal similarities with sites in eastern Africa (50, 51) and with age estimates from magnetochronology (49) and electron spin resonance (52).

KSD-VP-1/1 now throws substantial light on the natural history of hominid limb proportions (42), especially in conjunction with ARA-VP-6/500 (22). Only four other specimens preserve useful upper and lower limb elements. BOU-VP-1/1 (*ca*. 2.5 Ma, contemporary with *Au. garhi*) (53) and KNM-WT 15000 (*H. erectus*) (54) have modern human-like humerus/femur proportions, although BOU-VP-1/1 still exhibits a more elongate antebrachium than does *Homo*. Conclusions based on OH-62 (*H. habilis*) are unacceptably speculative (42).

Until now, therefore, only A.L. 288–1 has provided reliable *Au. afarensis* limb proportions (*SI Appendix*, Table S11). Because the crural index is stable in hominoids (80–85; *SI Appendix*, Table S12), its tibial length can be estimated from its nearly intact femur. Neither humerus nor antebrachial length is known for KSD-VP-1/1, but various forelimb joint dimensions are well preserved. As noted elsewhere, comparisons of fossil specimens should be made uniformly using direct metrics to avoid errors that result from estimating intermediate parameters such as body weight (43). We therefore will not revisit the debate about *Au. afarensis* limb proportions, because KSD-VP-1/1 provides direct linear data on upper limb joint size and lower limb length.

Fig. 5 compares tibia length with the geometric mean of eight measures of joint size in the humerus, ulna, and scapula. KSD-VP-1/1 falls well within the human distribution. This comparison might lead to the conclusion that the *Au. afarensis* tibia was as relatively elongate as those of modern humans. However, if the two specimens are assumed to be members of the same population, their positions in Fig. 5 suggest instead that the species probably exhibited a unique combination of lower limbs substantially longer than in an African ape of equivalent body size (*viz*., KSD-VP-1/1's forelimb joint size is more similar to that of *Pan* than to most *Homo*, but its hindlimb is much longer than that of *Pan*) and forelimbs more diminutive than in an African ape of equivalent body size (*viz*., A.L. 288–1's tibia length is similar to that of *Pan*, but its forelimb is far less robust). These observations are supported further by a comparison of individual articular dimensions and bone lengths in A.L. 288–1 and KSD-VP-1/1 treated separately (*SI Appendix*, Figs. S28–S30).

The estimated humerus/femur ratio in *Ar. ramidus* (ARA-VP-6/500) is 0.89 (22), similar to that of A.L. 288–1 (0.84) (*SI Appendix*, Table S11). Because the radius/tibia ratio and intermembral indexes of both *Ar. ramidus* and *Au. afarensis* also are close to those of *Proconsul* sp., it is most likely that the limb proportions of *Australopithecus* are simply primitive and that only moderate elongation of the hominid lower limb occurred thereafter (i.e., the *Homo* and *Australopithecus* distributions shown in Fig. 5 overlap substantially, but their mean values obviously are likely to have differed). The delay in the appearance of moderate hindlimb elongation as compared with the timing of numerous other adaptations to bipedality (8, 11, 14–16, 18–22) suggests that hindlimb elongation was of only limited adaptive significance.

Locomotor Pattern

KSD-VP-1/1 provides a unique opportunity to evaluate some aspects of the locomotor habitus of *Australopithecus.* As with A.L. 288–1, its total morphological pattern confirms well-established obligatory terrestrial bipedality with only minimal, if any, facultative exploitation of the arboreal environment. The scapula provides no evidence of a history of suspension or vertical climbing as it does in *Pan* (and to a lesser extent in *Gorilla*), and the thorax is more human- than ape-like. These characters are consistent with an ulna whose shaft is relatively straight, lacks a flexion tubercle (22), and exhibits an anterior-facing trochlear notch.

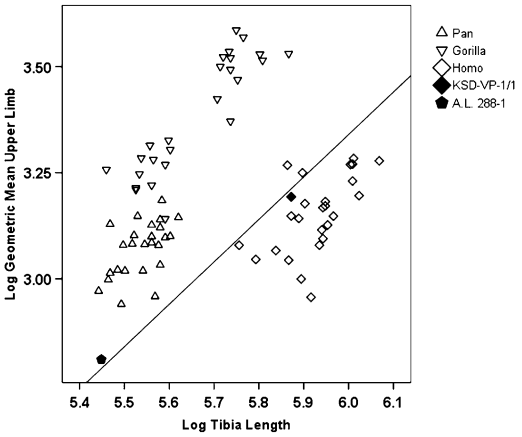

Fig. 5. Log-log scatterplot of tibia length versus upper limb size in KSD-VP-1/1 and A.L. 288–1. A.L. 288–1 tibia length from the mean crural index in hominoids (*SI Appendix*, Table S11). A reference line of slope equal to 1 is provided for reference (intercept = 2.66). Note that KSD-VP-1/1 and A.L. 288–1 fall close to this line, which passes through the human distribution.

The hindlimb of KSD-VP-1/1 reflects a virtual transformation of all elements to habitual bipedality, including a matrix of distal tibial features antithetical to vertical climbing (especially a deeply curved and mediolaterally narrow plafond) (18, 19), femoral characters indicative of a tibial dominant (14), valgus knee, and a pelvis with broad anteriorly extended abductor origins (16), a greatly shortened ischial ramus with an acutely angled tuberosity, a sacrum with distinctly broadened alae for emancipation of the lowest lumbars for full lordosis (55), a narrow, acute greater sciatic notch, a robust anterior inferior iliac spine arising from a unique separate center of ossification (indicative of novel, robust mediolateral expansion of the attachment of the anterior gluteals) (56), and deep iliopsoas and obturator externus tendon grooves (8, 12, 16). KSD-VP-1/1 now also confirms that some highly variable postcranial characters (e.g., "deficiency" of anterior lunate surface extension of the acetabulum), argued to indicate "facultative bipedality" (57), are, as previously noted (8), merely as variable in *Australopithecus* as in *Homo* and lack any locomotor valence (type 5). Even lower limb length, as now evidenced by KSD-VP-1/1, no longer remains an argument against "human-like" bipedal kinematics in *Au. afarensis* (58), because the distribution of relative lower limb length/relative forelimb size appears to have overlapped substantially with that of *Homo*. Moreover, judged in this manner, relative hindlimb length is likely to have been even more *Homo*-like than exhibited in Fig. 5, because the modern human forelimb (and thereby forelimb joint size) has been reduced substantially since *Au. afarensis* (42).

It has been argued that a proximal femur allocated to *Orrorin tugenensis* (BAR 1002'00) suggests an *Au. afarensis*-like locomotor pattern that persisted unchanged for several million years (59), although important femoral landmarks such as the shape and form of the greater trochanter are not fully preserved in BAR 1002'00. Moreover, data now available for *Ar. ramidus*, which postdates *O. tugenensis* by a considerable time period, make such locomotor stasis unlikely.

ANTHROPOLOGY

The total biomechanical pattern of *Au. afarensis* involves a host of specialized postcranial characters, all of which are fully consistent with data reported here for KSD-VP-1/1, those previously available for *Au. afarensis*, and the Laetoli footprints (58, 60), which at 3.66 Ma are just slightly older than KSD-VP-1/1 (61). Equally important are similarities between the *Au. afarensis* pelvis and the recently described *H. erectus* specimen from Busidima (BSN49/P27a–d) (11). These similarities are particularly striking, especially in light of the time separating them (at least 2.2 million years). Such constancy of morphotype suggests that highly derived terrestrial bipedality enjoyed a long period of stasis punctuated only occasionally by additional modifications to the postcranium of apparently decreasing selective significance (e.g., length of pedal intermediate phalanges, lower limb length).

ACKNOWLEDGMENTS. We thank R. S. Meindl for aid in interpreting our quantitative analyses, E. Russell for photography, and A. Ademassu for casting. We thank B. Rosenman, A. Ruth, and B. Hutchinson for metric data from specimens and computations. We thank J. DeSilva for data presented in the *SI Appendix*. We thank L. Jellema for help in collecting samples and preparation of X-rays. We thank P. Reno and M. A. McCollum for critical reading of the manuscript. We thank the Authority for Research and Conservation of Cultural Heritage and the National Museum of Ethiopia of the Ministry of Culture and Tourism for field and laboratory permissions and facilities. We thank the Afar Regional Government, its local administrative units, and the Afar people of Mille District for facilitating and participating in our research endeavors. We thank the Cleveland Museum of Natural History, Case Western Reserve University, and Berkeley Geochronology Center for access to comparative collections and laboratory use. This work was supported by Grants BCS-0234320, BCS-0542037, and BCS-0321893 from the National Science Foundation and by the Leakey Foundation, the Wenner-Gren Foundation, and the National Geographic Society.

1. Deino AL, et al. (2010) $^{(40)}$Ar/$^{(39)}$Ar dating, paleomagnetism, and tephrochemistry of Pliocene strata of the hominid-bearing Woranso-Mille area, west-central Afar Rift, Ethiopia. *J Hum Evol* 58:111–126.
2. Haile-Selassie Y, et al. (2007) Preliminary geology and paleontology of the Woranso-Mille, Central Afar, Ethiopia. *Anthropol Sci* 115:215–222.
3. Haile-Selassie Y, et al. (2010) New hominid fossils from Woranso-Mille (Central Afar, Ethiopia) and taxonomy of early *Australopithecus*. *Am J Phys Anthropol* 141:406–417.
4. Johanson DC, et al. (1982) Morphology of the Pliocene partial hominid skeleton (A.L. 288-1) from the Hadar Formation, Ethiopia. *Am J Phys Anthropol* 57:403–451.
5. Johanson DC, et al. (1978) A new species of the genus *Australopithecus* (Primates: Hominidae) from the Pliocene of eastern Africa. *Kirtlandia* 28:1–14.
6. Tague RG, Lovejoy CO (1998) A.L. 288-1—Lucy or Lucifer: Gender confusion in the Pliocene. *J Hum Evol* 35:75–94.
7. Häusler M, Schmid P (1995) Comparison of the pelves of Sts 14 and A.L. 288-1: Implications for birth and sexual dimorphism in australopithecines. *J Hum Evol* 29:363–383.
8. Lovejoy CO (2005) The natural history of human gait and posture. Part 1. Spine and pelvis. *Gait Posture* 21:95–112.
9. Lovejoy CO, et al. (2009) The pelvis and femur of *Ardipithecus ramidus*: The emergence of upright walking. *Science* 326 (71):71e1–71e6.
10. Lovejoy CO (1975) *Primate Morphology and Evolution*, ed Tuttle RH (Mouton, New York), pp 291–326.
11. Lovejoy CO, Heiple KG, Burstein AH (1973) The gait of *Australopithecus*. *Am J Phys Anthropol* 38:757–779.
12. Simpson SW, et al. (2008) A female *Homo erectus* pelvis from Gona, Ethiopia. *Science* 322:1089–1092.
13. Lovejoy CO (2007) *Movement, Stability, and Lumbopelvic Pain*, eds Vleeming A, Mooney V, Stoeckart R (Churchill Livingstone, London), pp 141–158.
14. Lovejoy CO (2007) The natural history of human gait and posture. Part 3. The knee. *Gait Posture* 25:325–341.
15. Lovejoy CO, Meindl RS, Ohman JC, Heiple KG, White TD (2002) The Maka femur and its bearing on the antiquity of human walking: Applying contemporary concepts of morphogenesis to the human fossil record. *Am J Phys Anthropol* 119:97–133.
16. Lovejoy CO (2005) The natural history of human gait and posture. Part 2. Hip and thigh. *Gait Posture* 21:113–124.
17. Wiltse LL (1972) Valgus deformity of the ankle: A sequel to the acquired or congenital abnormalities of the fibula. *J Bone Joint Surg Am* 54A:595–606.
18. DeSilva JM (2008) Vertical climbing adaptations in the anthropoid ankle and midfoot: Implications for locomotion in Miocene Catarrhines and Plio-Pleistocene Hominins. PhD thesis (Univ of Michigan, Ann Arbor, MI).
19. DeSilva JM (2009) Functional morphology of the ankle and the likelihood of climbing in early hominins. *Proc Natl Acad Sci USA* 106:6567–6572.
20. Lovejoy CO, et al. (2009) Careful climbing in the Miocene: The forelimbs of *Ardipithecus ramidus* and humans are primitive *Science* 326:70e1–70e8.
21. Latimer B, Ohman JC, Lovejoy CO (1987) Talocrural joint in African hominoids: Implications for *Australopithecus afarensis*. *Am J Phys Anthropol* 74:155–175.
22. Lovejoy CO, Suwa G, Simpson SW, Matternes JH, White TD (2009) The great divides: *Ardipithecus ramidus* reveals the postcrania of our last common ancestors with African apes. *Science* 326:100–106.
23. Latimer B, Ward CV (1993) *The Nariokotome Homo erectus Skeleton*, eds Walker AC, Leakey REF (Harvard Univ Press, Cambridge, MA), pp 266–293.
24. Jellema LM, Latimer B, Walker A (1993) *The Nariokotome Homo erectus Skeleton*, eds Walker AC, Leakey REF (Harvard Univ Press, Cambridge, MA), pp 294–325.
25. Schultz AH (1969) *The Life of Primates* (Universe Books, New York).
26. Vrba ES (1979) A new study of the scapula of *Australopithecus africanus* from Sterkfontein. *Am J Phys Anthropol* 51:117–129.
27. Alemseged Z, et al. (2006) A juvenile early hominin skeleton from Dikika, Ethiopia. *Nature* 443:296–301.
28. Hausler MF (2001) *New Insights into the Locomotion of Australopithecus africanus: Implications of the Partial Skeleton of Stw 431* (Univ of Zurich, Sterkfontein, South Africa).
29. Susman RL, Stern JT, Jungers WL (1984) Arboreality and bipedality in the Hadar hominids. *Folia Primatol (Basel)* 443:113–156.
30. Shea B (1986) Scapula form and locomotion in Chimpanzee evolution. *Am J Phys Anthropol* 70:475–488.
31. Inouye SE, Shea BT (1997) What's your angle: Size correction and bar-glenoid orientation in "Lucy" (A.L. 288-1). *Int J Primatol* 18:629–650.
32. Graves WWG (1921) The types of scapulae: A comparative study of some correlated characters in human scapulae. *Am J Phys Anthropol* 4:111–128.
33. Le Gros Clark WE (1978) *The Fossil Evidence for Human Evolution* (Univ. of Chicago Press, Chicago) 3rd Ed.
34. Fleagle JG, et al. (1981) Climbing: A biomechanical link with brachiation and with bipedalism. *Symposia of the Zoological Society of London.* 48:359–375.
35. Young N (2004) Modularity and integration in the hominoid scapula. *J Exp Zool B Mol Dev Evol* 302:226–240.
36. Lewin R, Foley RA (2004) *Principles of Human Evolution* (Blackwell, London), 2nd Ed.
37. White TD, et al. (1993) New discoveries of *Australopithecus* at Maka in Ethiopia. *Nature* 366:261–265.
38. Lovejoy CO, Johanson DC, Coppens Y (1982) Hominid upper limb bones recovered from the Hadar Formation: 1974–1977 collections. *Am J Phys Anthropol* 57:637–649.
39. Drapeau MS (2008) Articular morphology of the proximal ulna in extant and fossil hominoids and hominins. *J Hum Evol* 55:86–102.
40. Drapeau MS, Ward CV, Kimbel WH, Johanson DC, Rak Y (2005) Associated cranial and forelimb remains attributed to *Australopithecus afarensis* from Hadar, Ethiopia. *J Hum Evol* 48:593–642.
41. Drapeau MS (2004) Functional anatomy of the olecranon process in hominoids and Plio-Pleistocene hominins. *Am J Phys Anthropol* 124:297–314.
42. Reno PL, et al. (2005) Plio-Pleistocene hominid limb proportions. *Curr Anthropol* 46: 575–603.
43. Reno PL, Meindl RS, McCollum MA, Lovejoy CO (2003) Sexual dimorphism in *Australopithecus afarensis* was similar to that of modern humans. *Proc Natl Acad Sci USA* 100:9404–9409.
44. Rosenberg KR, Zune L, Ruff CB (2009) Body size, body proportions, and encephalization in a Middle Pleistocene archaic human from northern China. *Proc Natl Acad Sci USA* 103:3552–3556.
45. Jungers WL, Stern JT, Jr (1983) Body proportions, skeletal allometry and locomotion in the Hadar hominids: A reply to Wolpoff. *J Hum Evol* 12:673–684.
46. Wolpoff MH (1983) Lucy's little legs. *J Hum Evol* 12:443–453.
47. Pickering TR, Clarke RJ, Heaton JL (2004) The context of Stw 573, an early hominid skull and skeleton from Sterkfontein Member 2: Taphonomy and paleoenvironment. *J Hum Evol* 46:277–295.
48. Partridge TC, Granger DE, Caffee MW, Clarke RJ (2003) Lower Pliocene hominid remains from Sterkfontein. *Science* 300:607–612.
49. Walker J, Cliff RA, Latham AG (2006) U-Pb isotopic age of the StW 573 hominid from Sterkfontein, South Africa. *Science* 314:1592–1594.
50. Vrba ES (1995) *Paleoclimate and Evolution, with Emphasis on Human Origins,* (Yale Univ. Press, New Haven), pp 385–424.
51. Delson E (1988) *Evolutionary History of the "Robust" Australopithecines*, ed Grine FE (Aldine de Gruyter, Chicago), pp 317–324.
52. Curnoe D, Grün R, Taylor L, Thackeray F (2001) Direct ESR dating of a Pliocene hominin from Swartkrans. *J Hum Evol* 40:379–391.
53. Asfaw B, et al. (1999) *Australopithecus garhi*: A new species of early hominid from Ethiopia. *Science* 284:629–635.
54. Walker AC, Leakey REF (1993) *The Nariokotome Homo erectus Skeleton* (Harvard Univ Press, Cambridge, MA).
55. McCollum MA, et al. (2010) The vertebral formula of the last common ancestor of African apes and humans. *J Exp Zool B Mol Dev Evol* 314B:123–134.
56. Dart RA (1949) Innominate fragments of *Australopithecus prometheus*. *Am J Phys Anthropol* 7:301–333, illust.
57. Stern JT, Jr (2000) Climbing to the top: A personal memoir of *Australopithecus afarensis*. *Evol Anthropol* 9:113–133.
58. Raichlen DA, Gordon AD, Harcourt-Smith WEH, Foster AD, Haas WR, Jr (2010) Laetoli footprints preserve earliest direct evidence of human-like bipedal biomechanics. *PLoS ONE* 5:e9769 10.1371/journal.pone.0009769.
59. Richmond BG, Jungers WL (2008) *Orrorin tugenensis* femoral morphology and the evolution of hominin bipedalism. *Science* 319:1662–1665.
60. White TD, Suwa G (1987) Hominid footprints at Laetoli: Facts and interpretations. *Am J Phys Anthropol* 72:485–514.
61. Deino AL. 40Ar/39Ar dating of Laetoli, Tanzania. *Paleontology and Geology of Laetoli: Human Evolution in Context* (Springer) Vol 1: Geology, Geochronology, Paleoecology and Paleoenvironment, in press.